

Foothill: A Quasiconvex Regularization Function

Mouloud Belbahri, Eyyüb Sari, Sajad Darabi, Vahid Partovi Nia

Huawei Technologies Co., Ltd.
Montreal Research Center, Canada

Abstract

Deep neural networks (DNNs) have demonstrated success for many supervised learning tasks, ranging from voice recognition, object detection, to image classification. However, their increasing complexity yields poor generalization error. Adding noise to the input data or using a concrete regularization function helps to improve generalization. Here we introduce *foothill* function, an infinitely differentiable quasiconvex function. This regularizer is flexible enough to deform towards L_1 and L_2 penalties. Foothill can be used as a loss, as a regularizer, or as a binary quantizer.

1 Introduction

Deep learning has recently seen a surge in progress, from training shallow networks to very deep networks consisting of tens to hundreds of layers. Deep neural networks (DNNs) have demonstrated success for many supervised learning tasks (Szegedy et al., 2015; Simonyan and Zisserman, 2014). The focus has been on increasing accuracy, in particular for image, speech, and recently text tasks, where deep convolutional neural networks (CNNs) are applied. The resulting networks often include millions to billions parameters. Having too many parameters, increases the risk of over-fitting and hence a poor model generalization afterall.

Linear regression can be regarded as the simplest neural network, with no hidden layer and a linear activation function. Therefore, we start studying foothill in linear regression setting first. In the non-orthogonal setting, it is known that ordinary least squares estimators are inappropriate, specially in models with a large number of parameters. In another front, neural networks can be regarded as a nonparametric modeling with a lot of hidden states. In deep learning just like most nonparametric statistical models, the model fitted to the observed data is almost always wrong. Indeed, it does not represent the true generation of data. In order to be able to control the complexity of a model, it is not enough to just find the model of the right size, that is, the right number of parameters. In fact, the most appropriate model, in the sense of minimizing the generalization error, is almost always a penalized model in the right way to reduce the variance appropriately.

In the context of linear regression, the effectiveness of regularization has been supported practically and theoretically in several studies. In order to decrease the mean squared error of least squares estimates, ridge regression (Hoerl and Kennard, 1970) is proposed as a bias and variance trade-off by adding an L_2 regularization term to the least squares loss. The well-known lasso penalty is an L_1 regularization which sets some of the coefficients to zero (sparse selection) while shrinking the rest. The elastic net penalty (Zou and Hastie, 2005) linearly combines the L_1 and L_2 norms to provide a better generalization error in the

presence of co-linear features. Other regularizations such as SCAD (Fan and Li, 2001) have interesting theoretical properties such as sparse consistency and estimation consistency. However in deep learning regularization is sometimes hidden in heuristic methods during training. For instance dropout (Srivastava et al., 2014) is a widely-used method for addressing the problem of over-fitting. The idea is to drop units randomly from the neural network during training. It is known that dropout improves the test accuracy compared to standard regularizers such as L_1 (Tibshirani, 1996) and L_2 (Srivastava et al., 2014). Wager et al. (2013) proved that dropout is equivalent to an L_2 -type regularizer applied after scaling the inputs. Heuristic regularization is not limited to dropout only. Adding noise to the input data also yields lead to generalization error improvement (Bishop, 1995; Rifai et al., 2011). Data augmentation, and early stopping are some other heuristic regularizations widely applied in practice.

Inspired by the extensive research literature on regularization in the statistical community we introduce *foothill* as a quasiconvex function with attractive properties with strong potentials to be applied in practice in linear regression, robust estimation, curve estimation, training neural networks, and neural network quantization.

This function is a generalization of lasso and ridge penalties and has a strong potential to be used in deep learning. First, we start studying attractive functional properties of foothill that motivates its use in regularized linear models. Then, we demonstrate its application in other settings such as neural network training and neural network binary quantization. Foothill is flexible enough to be used as a regularizer or even as a loss function.

2 Foothill Regularizer

Let us define the mathematical notation first. Denote univariate variables with lowercase letters, e.g. x , vectors with lowercase and bold letters, e.g. \mathbf{x} , and matrices with uppercase and bold letters, e.g. \mathbf{X} .

2.1 Definition

Define the foothill regularization function as

$$p_{\alpha,\beta,\mu}(x) = \alpha(x - \mu) \tanh \left\{ \frac{\beta(x - \mu)}{2} \right\},$$

where $\tanh(\cdot)$ is the hyperbolic tangent function, $\alpha > 0$ is a shape parameter, $\beta > 0$ is a scale parameter and μ a location parameter. The function is symmetric about μ (see Figure 1). For the rest of the paper, set $\mu = 0$

$$p_{\alpha,\beta}(x) = \alpha x \tanh \left(\frac{\beta x}{2} \right). \tag{1}$$

The first and the second derivatives of the regularization function (see Figure 2) are

$$\frac{dp_{\alpha,\beta}(x)}{dx} = \alpha \tanh \left(\frac{\beta x}{2} \right) + \frac{1}{2} \alpha \beta x \operatorname{sech}^2 \left(\frac{\beta x}{2} \right),$$

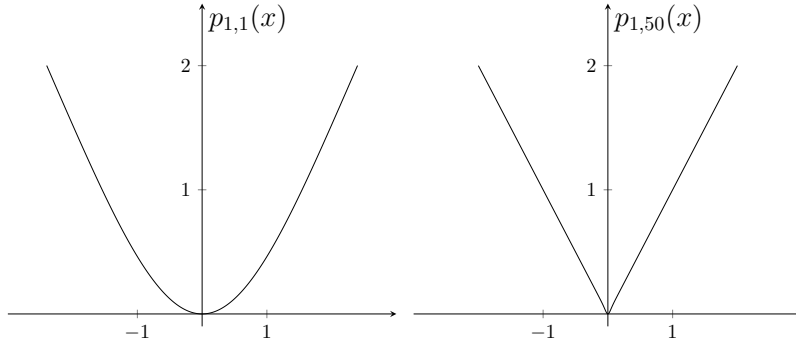


Figure 1: Regularization function for $\alpha = 1$, $\beta = 1$ (left panel) and $\alpha = 1$, $\beta = 50$ (right panel). The location parameter is set to $\mu = 0$.

$$\frac{d^2 p_{\alpha,\beta}(x)}{d^2 x} = \frac{1}{2} \alpha \beta \operatorname{sech}^2 \left(\frac{\beta x}{2} \right) \left\{ 2 - \beta x \tanh \left(\frac{\beta x}{2} \right) \right\},$$

where $\operatorname{sech}(\cdot)$ is the hyperbolic secant function.

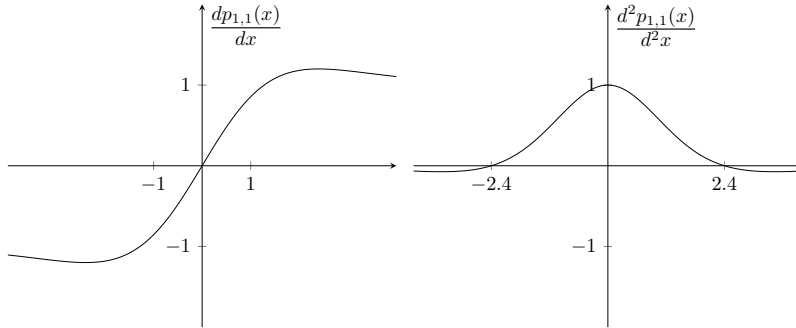


Figure 2: The first (left panel) and the second (right panel) derivatives of the regularization function (1) for $\alpha = 1$ and $\beta = 1$.

2.2 Properties

The regularization function (1) has several interesting properties. It is infinitely differentiable and symmetric about the origin,

$$p_{\alpha,\beta}(x) = p_{\alpha,\beta}(-x).$$

Also, it is flexible enough to approximate the lasso (Tibshirani, 1996) and Ridge penalties (Hoerl and Kennard, 1970) for particular values of α and β . The following properties suggest that this function could be considered as a quasiconvex alternative to the elastic net penalty (Zou and Hastie, 2005).

Property 1 For $\alpha = 1$ and $\beta \rightarrow \infty$, the standard penalty (1) converges to the lasso penalty.

Proof. For $x > 0$, it is easy to see that

$$\begin{aligned} \lim_{\beta \rightarrow +\infty} \tanh\left(\frac{\beta x}{2}\right) &= 1, \\ \lim_{\beta \rightarrow +\infty} p_{\alpha, \beta}(x) &= x. \end{aligned}$$

Equivalently, for negative x , as $p_{\alpha, \beta}(x)$ is symmetric about the origin, $\lim_{\beta \rightarrow +\infty} p_{\alpha, \beta}(x) = -x$, which is equivalent to $p_{\alpha, \beta}(x) \rightarrow |x|$ when $\beta \rightarrow +\infty$.

Property 2 For $\alpha > 0$, $\beta > 0$, and $\beta = 2/\alpha$ the standard penalty (1) approximates the Ridge penalty in a given interval $[-c; c]$.

Proof. Let us study this property formally. Take the Taylor expansion of (1),

$$p_{\alpha, \beta}(x) \approx \frac{\alpha\beta}{2}x^2 - \frac{\alpha\beta^3}{24}x^4 + \frac{\alpha\beta^5}{240}x^6 + O(x^8). \quad (2)$$

And, for a given $c > 0$,

$$\int_0^c \left(\frac{\alpha\beta}{2}x^2 - p_{\alpha, \beta}(x)\right)^2 dx \approx \frac{\alpha^2\beta^6}{5184}c^9 + O(c^{11}). \quad (3)$$

The integral in (3) diverges if c tends to infinity, but for a finite positive number c , one can numerically estimate the minimal distance between the L_2 norm and (1) with a tiny approximation error. This can be achieved by taking $\beta = 2/\alpha$ and (3) becomes

$$\int_0^c (x^2 - p_{\alpha, \beta}(x))^2 dx \approx \frac{1}{81\alpha^4}c^9 + O(c^{11}) = \varepsilon_c. \quad (4)$$

For large values of α , the error ε_c is negligible, see for example Figure 3 where the regularization function (1) approximates the Ridge penalty almost perfectly within $[-5; 5]$.

Further more, for fixed parameters, note that

$$\begin{aligned} \lim_{x \rightarrow +\infty} p_{\alpha, \beta}(x) - \alpha x &= 0, \\ \lim_{x \rightarrow -\infty} p_{\alpha, \beta}(x) + \alpha x &= 0. \end{aligned}$$

Hence it is also interesting to note that (1) acts like a polynomial function for small values of x , and like a linear function for large values. Therefore, using it as a loss function (instead of a regularization), (1) behaves like the Huber loss used in practice for robust estimation (Huber et al., 1964). Figure 3 shows that (1) is always bounded between the Huber loss and the squared error loss.

Property 3 Saddle points of $p_{\alpha, \beta}(x)$ are $x_0 \approx \pm 2.3994/\beta$ and $p_{\alpha, \beta}(x_0) = \frac{2\alpha}{\beta}$.

Proof. Indeed, the second order derivative vanishes at

$$2 - \beta x \tanh\left(\frac{\beta x}{2}\right) = 0,$$

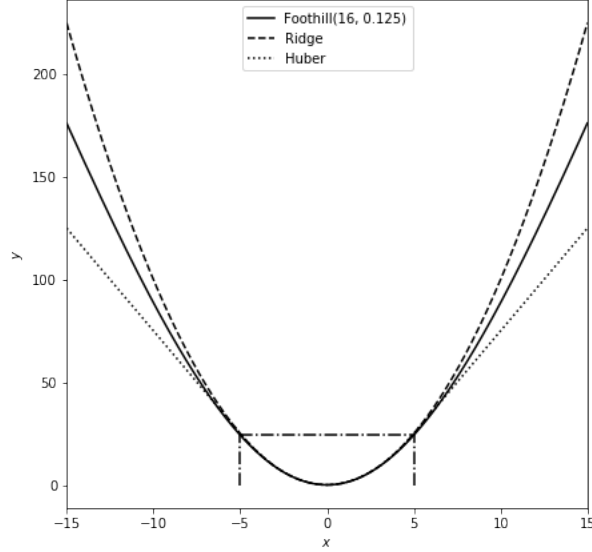


Figure 3: Plots of the Ridge, the Foothill penalty with $\alpha = 16$ and $\beta = 1/8$ and twice the Huber loss. The solid line represents the Foothill penalty, the dashed line represents the Ridge one (upper bound) and Huber (lower bound) is represented in dotted line.

which is solved by an iterative method for $\beta x \approx \pm 2.3994$. This implies

$$\beta x_0 \tanh\left(\frac{\beta x_0}{2}\right) = 2,$$

or equivalently

$$p_{\alpha,\beta}(x_0) = \frac{2\alpha}{\beta}.$$

Property 4 *The function $p_{\alpha,\beta}(x)$ is quasiconvex.*

Proof. It is straight forward to show that $p_{\alpha,\beta}(x)$ is decreasing from $-\infty$ to 0 and increasing from 0 to $+\infty$ and any monotonic function is quasiconvex (see Figure 2 left panel).

Table 1 suggests that the proposed function has the flexibility to be used for feature selection regularizer such as the lasso or used only to shrink the estimator in order to prevent overfitting like the Ridge. Finally, it also can be used as a loss function for robust regression as an alternative to the Huber loss.

3 Models

We start with motivating the properties of foothill regularizer in linear regression. Then, we discuss its use in neural networks and especially for binary quantization.

Table 1: Relationship to other functions

	Shape α	Scale β	Function
Lasso	1	$+\infty$	$p_{\alpha,\beta}(x) = x $
Ridge	$+\infty$	$2/\alpha$	$p_{\alpha,\beta}(x) = x^2$
Huber	$< +\infty$	$2/\alpha$	$p_{\alpha,\beta}(x) = \alpha x \tanh\left(\frac{x}{\alpha}\right)$
Foothill	1	2	$p_{\alpha,\beta}(x) = x \tanh(x)$

3.1 Regression

Suppose the response variable is measured with an additive statistical error ε and the relationship between the response and the predictors is fully determined by a smooth function

$$y_i = f(\mathbf{x}_i) + \varepsilon_i.$$

Initially suppose f is a linear function

$$y_i = \mathbf{x}_i^\top \boldsymbol{\theta} + \varepsilon_i.$$

Motivated from linear regression, one may re-write the model in matrix format

$$\mathbf{y} = \mathbf{X}\boldsymbol{\theta} + \boldsymbol{\varepsilon}, \tag{5}$$

where $\mathbf{y}_{n \times 1}$ is the vector of observed response, $\mathbf{X}_{n \times p}$ is row-wise stacked matrix of predictors, $\boldsymbol{\theta}_{p \times 1}$ is the p -dimensional vector of coefficients, and $\boldsymbol{\varepsilon}_{n \times 1}$ is white noise with zero mean and a constant variance τ^2 .

The penalized estimator with squared-loss function is defined as

$$\hat{\boldsymbol{\theta}} = \underset{\boldsymbol{\theta}}{\operatorname{argmin}} \frac{1}{2n} \|\mathbf{y} - \mathbf{X}\boldsymbol{\theta}\|_2^2 + \lambda \sum_{j=1}^p p_{\alpha,\beta}(\theta_j), \tag{6}$$

where $p_{\alpha,\beta}(\cdot)$ is the standard regularization function (1). Here, λ is the regularization constant. Setting $\lambda = 0$ returns the ordinary least squares estimates, which performs no shrinking and no selection. For a given $\lambda > 0$ and finite α and β , the regression coefficients $\hat{\boldsymbol{\theta}}$ are shrunk towards zero, and for $\alpha = 1$, when $\beta \rightarrow +\infty$, (1) converges to the lasso penalty which sets some of the coefficients to zero (sparse selection), so does selection and shrinkage simultaneously.

To gain more insight about the proposed penalty, we consider the orthogonal case where we assume that the columns of \mathbf{X} in (5) are orthonormal, i.e. $\mathbf{X}^\top \mathbf{X} = n\mathbf{I}_p$. Therefore, the minimization problem of (6) is equivalent to estimating coefficients component-wise. Let $\hat{z}_j = \mathbf{x}_j^\top \mathbf{y}/n$ be the ordinary least squares estimate for $j = 1, \dots, p$. Here, for fixed $\alpha > 0$ and a given scale parameter $\beta > 0$, this leads us to the univariate optimization problem

$$\underset{\theta_j}{\operatorname{argmin}} \left[\frac{1}{2}(\hat{z}_j - \theta_j)^2 + \lambda \alpha \theta_j \tanh\left(\frac{\beta \theta_j}{2}\right) \right]. \tag{7}$$

The numerical solutions of (7) with various values of α and β are shown in Figure 4. When β is small, the solutions are smooth and by increasing β , the solutions become similar to ones of lasso, but still with a smoothness that lasso does not have.

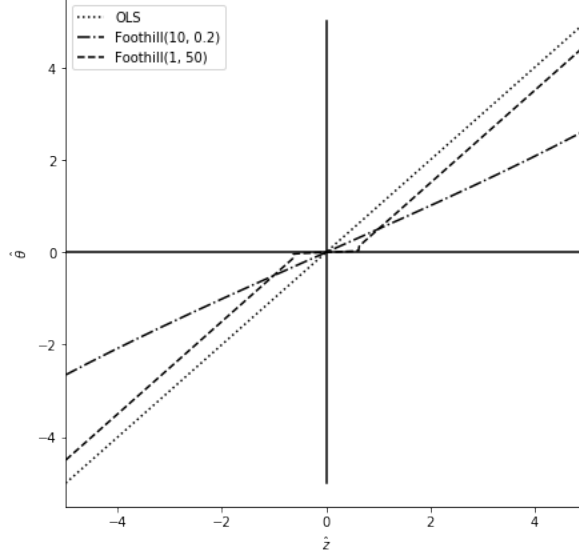


Figure 4: Plots of the solution paths in orthogonal design study according to the least squares estimator \hat{z} for the foothill regularization with $\alpha = 10$ and $\beta = 0.2$ (dashed and dotted line) and $\alpha = 1$ and $\beta = 50$ (dashed line), with $\lambda = 0.5$. The dotted line represents the least squares estimator \hat{z} .

Following Knight and Fu (2000) proof for Bridge regression (Frank and Friedman, 1993), we show that under similar conditions (but a fixed λ), the penalized estimator is \sqrt{n} -consistent. Consider the linear model (5) and denote the penalized least squares function by

$$J_n(\boldsymbol{\theta}) = \frac{1}{2}(\mathbf{y} - \mathbf{X}\boldsymbol{\theta})^\top(\mathbf{y} - \mathbf{X}\boldsymbol{\theta}) + \lambda \sum_{j=1}^p p_{\alpha,\beta}(\theta_j).$$

Property 5 Assume that the matrix $\mathbb{E}[\mathbf{X}^\top \mathbf{X}] < \infty$ is positive definite. Let $\hat{\boldsymbol{\theta}}_n$ be the penalized estimator. $\hat{\boldsymbol{\theta}}_n$ is consistent if any given $\epsilon > 0$, there exist a large constant C such that

$$\Pr \left(\inf_{\|\mathbf{u}\|=C} J_n \left(\boldsymbol{\theta} + \frac{\mathbf{u}}{\sqrt{n}} \right) > J_n(\boldsymbol{\theta}) \right) \geq 1 - \epsilon. \quad (8)$$

Proof. This implies there is a local minimizer such that $\|\hat{\boldsymbol{\theta}}_n - \boldsymbol{\theta}\| = O_P(\sqrt{n})$. Simple algebra

shows that

$$\begin{aligned} D_n(\mathbf{u}) &:= J_n(\boldsymbol{\theta} + \frac{\mathbf{u}}{\sqrt{n}}) - J_n(\boldsymbol{\theta}) \\ &= \frac{1}{2} \mathbf{u}^\top \frac{\mathbf{X}^\top \mathbf{X}}{n} \mathbf{u} - \mathbf{u}^\top \frac{\mathbf{X}^\top (\mathbf{y} - \mathbf{X}\boldsymbol{\theta})}{\sqrt{n}} \\ &\quad + \lambda \sum_{j=1}^p \left(p_{\alpha,\beta} \left(\theta_j + \frac{u_j}{\sqrt{n}} \right) - p_{\alpha,\beta}(\theta_j) \right), \end{aligned}$$

which is minimized at $\sqrt{n}(\hat{\boldsymbol{\theta}}_n - \boldsymbol{\theta})$. By the strong law of large numbers and the central limit theorem, the first two terms converge to

$$\frac{1}{2} \mathbf{u}^\top \mathbb{E}[\mathbf{X}^\top \mathbf{X}] \mathbf{u} - \mathbf{u}^\top \mathbf{Z},$$

where $\mathbf{Z} \sim \mathcal{N}(\mathbf{0}, \boldsymbol{\Sigma})$ where $\boldsymbol{\Sigma} = \tau^2 \mathbb{E}[\mathbf{X}^\top \mathbf{X}]$. The third term can be rewritten as

$$\frac{\lambda}{\sqrt{n}} \sum_{j=1}^p \left(\frac{p_{\alpha,\beta} \left(\theta_j + \frac{u_j}{\sqrt{n}} \right) - p_{\alpha,\beta}(\theta_j)}{\frac{u_j}{\sqrt{n}}} \right) u_j,$$

and suppose that $\frac{\lambda}{\sqrt{n}} \rightarrow \lambda_0$. Therefore, when $n \rightarrow +\infty$, we have $\frac{u_j}{\sqrt{n}} \rightarrow 0$ so the third term of D_n converges to

$$\lambda_0 \sum_{j=1}^p \left(\frac{dp_{\alpha,\beta}(\theta_j)}{d\theta_j} \right) u_j.$$

For λ fixed, $\lambda_0 = 0$ and the first derivative of the standard regularization function is bounded, which means that $D_n(\mathbf{u})$ converges to

$$D(\mathbf{u}) = \frac{1}{2\tau^2} \mathbf{u}^\top \boldsymbol{\Sigma} \mathbf{u} - \mathbf{u}^\top \mathbf{Z},$$

which is convex and has a unique minimizer and hence,

$$\sqrt{n}(\hat{\boldsymbol{\theta}}_n - \boldsymbol{\theta}) \rightarrow_d \operatorname{argmin} D(\mathbf{u}),$$

which shows that by choosing sufficiently large C , (8) holds and that $\hat{\boldsymbol{\theta}}_n$ is \sqrt{n} -consistent.

3.2 Neural Networks

The regularization term is added to the loss function,

$$J(\mathbf{W}, \mathbf{b}) = L(\mathbf{W}, \mathbf{b}) + \lambda \sum_{h=1}^H p_{\alpha,\beta}(\mathbf{W}_h), \quad (9)$$

where $L(\mathbf{W}, \mathbf{b})$ is the cost function, \mathbf{W} and \mathbf{b} are the matrices of all weights and bias parameters in the network, \mathbf{W}_h is the matrix of weights at layer h and H is the total number of layers. Here, $p_{\alpha,\beta}(\cdot)$ is the regularization function (1). The regularization function is

differentiable, so more convenient to implement in back-propagation. The parameters α and β could be defined for the whole network or per layer. In this case, each layer have its own regularization term.

It is hard to deploy deep neural networks models on low-end edge devices which have tight resource constraints in memory size or battery life. Quantization is an effective approach to satisfy these constraints. Instead of working with full-precision values to represent the parameters and activations, quantized representations use more compact formats such as integers or binary numbers.

Often, binary neural networks (BNN) are trained with heuristic methods (Courbariaux et al., 2015; Rastegari et al., 2016; Hubara et al., 2016). However it is possible to embed the loss function with an appropriate regularization to encourage binary training. Common regularizations encourage the weights to be estimated near zero. Such regularization are not aligned with the objective of training binary network where the weights are encouraged to be estimated -1 or $+1$. The framework of BNN+ (Darabi et al., 2018) introduces modified L_1 and L_2 regularizations functions which encourage the weights to concentrate around $\mu \times \{-1; +1\}$, where μ is a scaling factor. The modified L_1 and L_2 regularizations are defined as

$$R_1(x) = ||x| - \mu|, \tag{10}$$

$$R_2(x) = (|x| - \mu)^2. \tag{11}$$

We follow the same idea and modify (1) to construct a shifted regularization function $\tilde{p}_{\alpha,\beta}(x)$ as

$$\tilde{p}_{\alpha,\beta}(x) = p_{\alpha,\beta}(x - \mu \text{sign}(x)). \tag{12}$$

Training the objective function

$$L(\mathbf{W}, \mathbf{b}) + \lambda \sum_{h=1}^H \tilde{p}_{\alpha,\beta}(\mathbf{W}_h)$$

quantizes the weights around $\{-\mu; +\mu\}$ for large values of the regularization constant λ . Adding the regularization function to the objective function of a deep neural networks adds only one line to the back-propagation in order to estimate the scaling factors. Hence, while training, the regularization function adapts and the weights are encouraged towards $\mu \times \{-1; +1\}$ (see Figure 5). We suggest starting training with $\lambda = 0$ and increasing λ with logarithmic rate as a function of the number of epochs. The scaling factor and the number of scaling factors are important for BNN to compete with full-precision networks. In practice, we use a scaling factor per neuron for fully-connected layers and a scaling factor per filter for convolutional layers. Without a scaling factor, the accuracy loss is large (Courbariaux et al., 2015). The scaling factors are applied after the fully-connected and convolutional layers which are performed using xnor-popcount operations during inference. In our experiments, we train the scaling factors with back-propagation.

For a convex function there are no saddle points and all local minima are also global. Thus gradient descent, with a suitable learning rate, is guaranteed to find a global minimizer. The presence of saddle points and local minima makes non-convex optimization hard. Finding the global minimizer in such a setting is generally NP-hard. However, provided the step size is not chosen aggressively, the gradient method never converges to saddle points (Lee et al.,

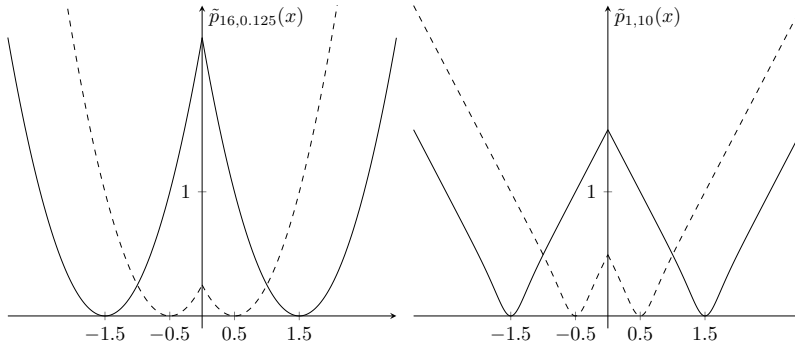


Figure 5: Regularization functions for binary networks (12) with $\alpha = 16$ and $\beta = 1/8$ (left panel) and $\alpha = 1$ and $\beta = 10$ (right panel). Dashed line is $\mu = 0.5$ and solid line is $\mu = 1.5$. The scaling factor μ is trainable, as a result the regularization function adapts accordingly.

2016). Greedy methods that use precise line search may still get stuck at stationary points but a small step gradient method will only converge to minimizers. The presence of saddle points might slow gradient descent progress down because directions of low curvature are exploited too slowly (Ge et al., 2015). However, the regularization function (1) has only two stationary points and based on our experiments, it is simple enough to be used with gradient descent.

4 Application

In this section, we evaluate the proposed regularizer on different applications. First, we study the prostate cancer data with the goal of showing that the elastic net penalty and the foothill penalty provide comparable performance. Second, we use the regularization function (1) as a loss function for robust estimation on simulated data. Then, we apply the function on classical neural networks architectures using MNIST and CIFAR-10 datasets. Finally, we use the shifted foothill regularization function (12) in order to quantize a neural network and train it on ImageNet dataset.

4.1 Regression

In this section, we aim to show that foothill function is flexible enough to be used as the L_1 , L_2 or the elastic net penalty, as well as the Huber loss function, in a regression context. We use a small dataset in order to show that using the foothill regularizer yields similar results to using the elastic net penalty. Then, on synthetic data, we show that the foothill loss function handles outliers as the Huber loss function does.

Prostate Cancer Data. We compare different regularized linear models on the prostate cancer data (Stamey et al., 1989). This small dataset contains 97 observations with eight explanatory variables (clinical measures) and a prostate-specific continuous response variable. The goal is to show that the regularization function (1) is an alternative to the elastic net penalty. In order to compare different models, we use 100 bootstrap replicates of the original dataset. We then split each replicate sample into 2/3 training and 1/3 validation observations.

We fit the different regularized linear models on the training sets and we compute the mean squared error (MSE) on the validation sets. Taking the average of the 100 validation MSE gives us a good measure of quality of fitted models. Recall the elastic net penalty

$$p_\delta(x) = (1 - \delta)x^2 + \delta|x|,$$

where $\delta \in [0; 1]$ makes the bridge between lasso and Ridge. We can see in Table 2 that the regularization function (1) gives similar results to the elastic net penalty on the prostate cancer data.

Table 2: Prostate cancer data: comparing different methods. The regularization function (1) and the elastic net penalty give similar results. The maximum standard error of the validation (Val.) MSE is 0.1, so it is not reported for each line.

Method	Parameter(s)	λ	Val. MSE ¹
Lasso	$\delta = 1$	0.03	0.397
Ridge	$\delta = 0$	0.08	0.397
Elastic Net	$\delta = 0.25$	0.05	0.396
	$\delta = 0.5$	0.04	0.396
	$\delta = 0.75$	0.03	0.397
Foothill	(α, β)		
Lasso-like	(1, 100)	3.05	0.398
	(1, 500)	4.10	0.393
	(1, 1000)	3.07	0.397
Ridge-like	(1000, 0.002)	5.00	0.384
	(500, 0.004)	4.85	0.394
	(100, 0.02)	4.31	0.396

Robust Regression. We investigate the finite sample performance of the proposed function (1) as a loss function through a numerical illustration. Consider a simple linear regression with three different losses. The goal is to compare the usual squared-error loss with the Huber and Foothill losses in presence of an outlier. The data is generated from a linear function

$$y_i = 0.5 + 1.5x_i + \varepsilon_i,$$

where $x_i \sim U[-5; 5]$ and $\varepsilon_i \sim \mathcal{N}(0, 1.5^2)$ for $i = 1, \dots, 50$.

We first fit the different models on the simulated data points in order to estimate the parameters. Then, we change one y_i value in order to create an outlier. We fit once again the three models and compute the new estimates. The fitted models are presented in Table 3 and Figure 6. This toy example suggests that the proposed loss function is more robust than the squared-error loss.

¹Mean squared error (MSE) computed by 3-fold cross-validation over 100 bootstrap replicate samples.

Table 3: Simple linear regression models on synthetic data with different loss functions: a) squared-error loss (Ridge), b) Huber loss and c) Foothill loss with $\alpha = 6$ and $\beta = 1/3$. The models are fitted twice: first, without outliers and second, with one outlier.

Method	Without outliers	With one outlier
Ridge	$\hat{y} = 0.5 + 1.46x$	$\hat{y} = 1.0 + 1.68x$
Huber	$\hat{y} = 0.6 + 1.46x$	$\hat{y} = 0.6 + 1.42x$
Foothill	$\hat{y} = 0.5 + 1.46x$	$\hat{y} = 0.6 + 1.46x$

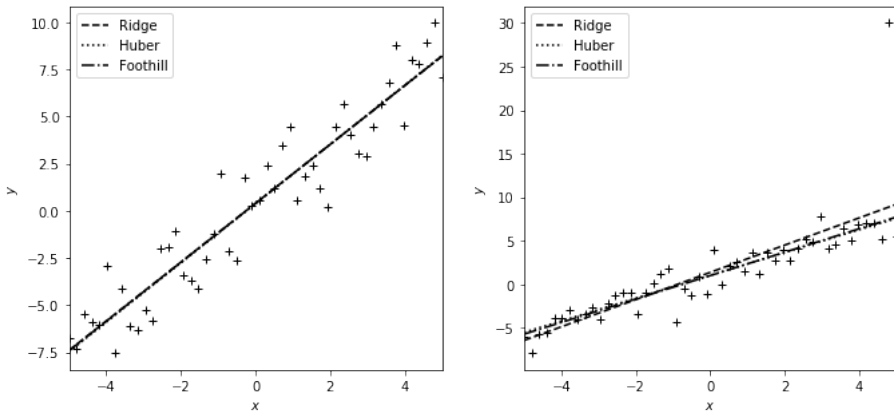


Figure 6: Simple linear regression models with different loss functions: a) squared-error loss (Ridge), b) Huber loss and c) Foothill loss with $\alpha = 6$ and $\beta = 1/3$. The left panel shows the fitted models on the synthetic data. They are almost identical. The right panel shows the fitted models on a data that has one outlier where foothill and Huber loss remain robust to the added outlier.

4.2 Neural Networks

For neural networks, we evaluate the performance of the foothill on two datasets. We first use the regularizer for digit classification task on MNIST dataset. Then, we compare the foothill regularizer to L_1 and L_2 on CIFAR-10 dataset. These experiments show that the foothill function can be a good flexible alternative to L_1 and L_2 .

Digit Classification. We use LeNet-5 (LeCun et al., 1998) architecture in order to compare Foothill (1) to L_1 and L_2 regularizers on the digit classification dataset MNIST. We train the network for 20 epochs using the ADAM (Kingma and Ba, 2014) optimizer at a learning rate of 10^{-3} , $\beta_1 = 0.9$, $\beta_2 = 0.999$ with regularization constant λ set to 10^{-4} and different combinations of α and β . Images were zero-padded to match 32x32 pixels, no data augmentation was performed. The results are summarized in Table 4.

Table 4 shows that using foothill regularizer, L_1 or L_2 yields to comparable accuracy. Because foothill is more flexible than L_1 and L_2 , we believe that it will help fine-tuning in order to get the right amount of regularization. Next, we compare the regularization functions on a

Table 4: Top-1 accuracies on MNIST test set, using the regularization function (1) with LeNet 5. The regularization constant λ is set to 10^{-4} .

Method	Test Accuracy
No Regularization	98.9%
$L_1(x)$	99.1%
$p_{1,500}(x)$	99.1%
$L_2(x)$	99.1%
$p_{100,0.02}(x)$	99.2%

harder task.

Image Classification. We use AlexNet architecture (Krizhevsky et al., 2012) augmented by batch normalization (Ioffe and Szegedy, 2015) in order to compare Foothill (1) to L_1 and L_2 regularizers on CIFAR-10. We train the network for 50 epochs using stochastic gradient descent (SGD) optimizer with momentum 0.9 and a learning rate of 10^{-2} that is divided by 10 at epochs 20 and 30. The regularization constant λ is fine-tuned for each regularizer. During training, images are resized to 256×256 and a random crop is applied to obtain 224×224 input size. Random horizontal flip is also used as a data augmentation technique. At test time, images are resized to 256×256 and a center crop is applied to get 224×224 size. For both steps, standardization is applied with mean = [0.485, 0.456, 0.406] and std = [0.229, 0.224, 0.225]. Note that before preprocessing, pixel values range in [0, 1]. The results are summarized in Table 5.

Table 5: AlexNet top-1 accuracies on CIFAR-10 test set, using L_1 , L_2 and Foothill (1) with different λ values. Top-1 accuracy for non-regularized AlexNet is 88.63%.

Method	$\lambda = 10^{-4}$	$\lambda = 10^{-3}$	$\lambda = 10^{-2}$
$L_1(x)$	89.75%	81.74%	55.59%
$p_{0.5,50}(x)$	89.53%	90.55%	85.60%
$p_{0.75,50}(x)$	90.24%	90.05%	84.78%
$L_2(x)$	88.61%	89.51%	89.99%
$p_{16,0.125}(x)$	88.73%	89.30%	89.86%
$p_{20,0.1}(x)$	89.12%	89.44%	90.21%
$p_{100,0.02}(x)$	88.99%	89.79%	89.92%

The results reported in Table 5 empirically demonstrate the flexibility of Foothill against L_1 and L_2 . Our regularization function is less sensitive to the choice of λ , for instance L_1 -regularized AlexNet’s accuracy can have 34.16% difference depending on which λ has

been used for training while $p_{0.5,50}$ -regularized AlexNet’s accuracy difference ranges in 4.96%. Our hypothesis is further more validated on an extreme case, binary quantization.

4.3 Binary Quantization

We quantize AlexNet architecture using the shifted foothill regularization function from equation (12) on ILSVRC 2012 (ImageNet). This dataset consists of ~ 1.2 M training images, 50K validation images and 1000 classes. The data preprocessing pipeline is the same as for CIFAR-10 experiments. Batch normalization layers are added to the architecture. The weights and activations are quantized using the sign function for all convolutional and fully-connected layers except the first and the last one which are kept to be in full-precision. We initialize the learning rate with 5×10^{-3} and divide it each 10 epochs alternatively, by 5 and by 2.

We compare our method to traditional binary networks and Table 6 summarizes the results. We use $\lambda = 10^{-6} \times \log(t)$ where t is the current epoch and train the networks for 100 epochs.

Table 6: Comparison of top-1 and top-5 accuracies of quantized neural network using the lasso (10), ridge (11) and foothill (12) modified regularizers to traditional BinaryNet (Hubara et al., 2016) and XNOR-Net (Rastegari et al., 2016) on ImageNet dataset, using AlexNet architecture.

Method	Top-1 Accuracy	Top-5 Accuracy
$R_1(x)$	43.0%	67.5%
$\tilde{p}_{0.5,50}(x)$	44.4%	68.5%
$\tilde{p}_{0.75,50}(x)$	44.3%	68.4%
$R_2(x)$	42.9%	67.5%
$\tilde{p}_{100,0.02}(x)$	44.2%	68.5%
$\tilde{p}_{20,0.1}(x)$	44.5%	68.3%
BinaryNet	41.2%	65.6%
XNOR-Net	44.2%	69.2%
Full-Precision	57.1%	80.3%

In Table 6, we report XNOR-Net performance from the original paper of Rastegari et al. (2016) and the BinaryNet one from the implementation of Lin et al. (2017), which is higher than the one reported in the original paper. We do not report the performance of Darabi et al. (2018) as they make use of a pre-trained model in their experiments, whereas we train the binary neural networks from scratch. We see that quantizing a neural network using foothill function as a regularization that pushes the weights towards binary values gives more accurate results for ImageNet dataset, better than L_1 and L_2 by more than 1.5%. Furthermore, for AlexNet architecture, our method beats the state of the art BinaryNet and XNOR-Net by the margin 3.3% and 0.3% respectively.

5 Discussion

Here we developed a new function, called foothill, that can be used as a loss function, or as a regularizer, or a binary quantizer.

As a loss function, the behaviour of foothill is similar to the Huber loss.

As a regularizer foothill may encourage estimation shrinkage, sparse selection, or both depending on the values of its parameters. More concretely its parameters can be tuned to approximate both lasso (which implements sparse selection) and ridge penalty (which implements shrinkage). Therefore foothill looks like a quasiconvex version of the elastic net which approximates the lasso and the ridge.

Most of the deep networks includes millions of parameters that requires extensive resources to be implemented in realtime. A modified version of foothill can be used to quantize deep networks and ultimately run neural networks to low power edge devices, such as wearable devices, cell phones, wireless base stations, etc. Network quantization yields to accuracy degradation. Recent studies (Courbariaux et al., 2015; Hubara et al., 2016; Rastegari et al., 2016) suggest proper training of weights controls the accuracy loss. The shift version of foothill has the potential of pushing heuristic training more towards a more clear and formalized training using regularization. Our numerical results confirm this assumption since our implementation of a quantized neural network using foothill regularizer beats L_1 and L_2 regularizers and XNOR-Net, which is the state of the art binary quantization method.

References

- Bishop, C. M. (1995). Training with noise is equivalent to tikhonov regularization. *Neural Computation*, 7(1):108–116.
- Courbariaux, M., Bengio, Y., and David, J.-P. (2015). Binaryconnect: Training deep neural networks with binary weights during propagations. In *Advances in neural information processing systems*, pages 3123–3131.
- Darabi, S., Belbahri, M., Courbariaux, M., and Nia, V. P. (2018). BNN+: Improved binary network training. *arXiv preprint arXiv:1812.11800*.
- Fan, J. and Li, R. (2001). Variable selection via nonconcave penalized likelihood and its oracle properties. *Journal of the American Statistical Association*, 96(456):1348–1360.
- Frank, L. E. and Friedman, J. H. (1993). A statistical view of some chemometrics regression tools. *Technometrics*, 35(2):109–135.
- Ge, R., Huang, F., Jin, C., and Yuan, Y. (2015). Escaping from saddle points online stochastic gradient for tensor decomposition. In *Conference on Learning Theory*, pages 797–842.
- Hoerl, A. E. and Kennard, R. W. (1970). Ridge regression: Biased estimation for nonorthogonal problems. *Technometrics*, 12(1):55–67.
- Hubara, I., Courbariaux, M., Soudry, D., El-Yaniv, R., and Bengio, Y. (2016). Binarized neural networks. In *Advances in Neural Information Processing Systems*, pages 4107–4115.
- Huber, P. J. et al. (1964). Robust estimation of a location parameter. *The Annals of Mathematical Statistics*, 35(1):73–101.

- Ioffe, S. and Szegedy, C. (2015). Batch normalization: Accelerating deep network training by reducing internal covariate shift. *arXiv preprint arXiv:1502.03167*.
- Kingma, D. P. and Ba, J. (2014). Adam: A method for stochastic optimization. *arXiv preprint arXiv:1412.6980*.
- Knight, K. and Fu, W. (2000). Asymptotics for lasso-type estimators. *Annals of Statistics*, pages 1356–1378.
- Krizhevsky, A., Sutskever, I., and Hinton, G. E. (2012). Imagenet classification with deep convolutional neural networks. In *Advances in Neural Information Processing Systems*, pages 1097–1105.
- LeCun, Y., Bottou, L., Bengio, Y., and Haffner, P. (1998). Gradient-based learning applied to document recognition. *Proceedings of the IEEE*, 86(11):2278–2324.
- Lee, J. D., Simchowitz, M., Jordan, M. I., and Recht, B. (2016). Gradient descent converges to minimizers. *arXiv preprint arXiv:1602.04915*.
- Lin, X., Zhao, C., and Pan, W. (2017). Towards accurate binary convolutional neural network. In *Advances in Neural Information Processing Systems*, pages 345–353.
- Rastegari, M., Ordonez, V., Redmon, J., and Farhadi, A. (2016). Xnor-net: Imagenet classification using binary convolutional neural networks. In *European Conference on Computer Vision*, pages 525–542. Springer.
- Rifai, S., Glorot, X., Bengio, Y., and Vincent, P. (2011). Adding noise to the input of a model trained with a regularized objective. *arXiv preprint arXiv:1104.3250*.
- Simonyan, K. and Zisserman, A. (2014). Very deep convolutional networks for large-scale image recognition. *arXiv preprint arXiv:1409.1556*.
- Srivastava, N., Hinton, G., Krizhevsky, A., Sutskever, I., and Salakhutdinov, R. (2014). Dropout: a simple way to prevent neural networks from overfitting. *The Journal of Machine Learning Research*, 15(1):1929–1958.
- Stamey, T. A., Kabalin, J. N., McNeal, J. E., Johnstone, I. M., Freiha, F., Redwine, E. A., and Yang, N. (1989). Prostate specific antigen in the diagnosis and treatment of adenocarcinoma of the prostate. ii. radical prostatectomy treated patients. *The Journal of Urology*, 141(5):1076–1083.
- Szegedy, C., Liu, W., Jia, Y., Sermanet, P., Reed, S., Anguelov, D., Erhan, D., Vanhoucke, V., and Rabinovich, A. (2015). Going deeper with convolutions. In *Proceedings of the IEEE conference on computer vision and pattern recognition*, pages 1–9.
- Tibshirani, R. (1996). Regression shrinkage and selection via the lasso. *Journal of the Royal Statistical Society: Series B*, pages 267–288.
- Wager, S., Wang, S., and Liang, P. S. (2013). Dropout training as adaptive regularization. In *Advances in Neural Information Processing Systems*, pages 351–359.
- Zou, H. and Hastie, T. (2005). Regularization and variable selection via the elastic net. *Journal of the Royal Statistical Society: Series B*, 67(2):301–320.